



**Universiteit  
Leiden**  
The Netherlands

## **Blood-brain barrier leakage and microvascular lesions in cerebral amyloid angiopathy**

Freeze, W.M.; Bacskai, B.J.; Frosch, M.P.; Jacobs, H.I.L.; Backes, W.H.; Greenberg, S.M.; Veluw, S.J. van

### **Citation**

Freeze, W. M., Bacskai, B. J., Frosch, M. P., Jacobs, H. I. L., Backes, W. H., Greenberg, S. M., & Veluw, S. J. van. (2019). Blood-brain barrier leakage and microvascular lesions in cerebral amyloid angiopathy. *Stroke*, 50(2), 328-335. doi:10.1161/STROKEAHA.118.023788

Version: Publisher's Version  
License: [Creative Commons CC BY 4.0 license](https://creativecommons.org/licenses/by/4.0/)  
Downloaded from: <https://hdl.handle.net/1887/3630344>

**Note:** To cite this publication please use the final published version (if applicable).

# Blood-Brain Barrier Leakage and Microvascular Lesions in Cerebral Amyloid Angiopathy

Whitney M. Freeze, PhD; Brian J. Bacsikai, PhD; Matthew P. Frosch, MD PhD;  
Heidi I.L. Jacobs, PhD; Walter H. Backes, PhD; Steven M. Greenberg, MD PhD;  
Susanne J. van Veluw, PhD

**Background and Purpose**—Cerebral amyloid angiopathy (CAA) is a common small vessel disease that independently affects cognition in older individuals. The pathophysiology of CAA and CAA-related bleeding remains poorly understood. In this postmortem study, we explored whether blood-brain barrier leakage is associated with CAA and microvascular lesions.

**Methods**—Eleven CAA cases (median [IQR] age=69 years [65–79 years], 8 males) and 7 cases without neurological disease or brain lesions (median [IQR] age=77 years [68–92 years], 4 males) were analyzed. Cortical sections were sampled from each lobe, and IgG and fibrin extravasation (markers of blood-brain barrier leakage) were assessed with immunohistochemistry. We hypothesized that IgG and fibrin extravasation would be increased in CAA cases compared with controls, that this would be more pronounced in parietooccipital brain regions compared with frontotemporal brain regions in parallel with the posterior predilection of CAA, and would be associated with CAA severity and number of cerebral microbleeds and cerebral microinfarcts counted on ex vivo magnetic resonance imaging of the intact brain hemisphere.

**Results**—Our results demonstrated increased IgG positivity in the frontotemporal ( $P=0.044$ ) and parietooccipital ( $P=0.001$ ) cortex in CAA cases compared with controls. Within CAA cases, both fibrin and IgG positivity were increased in parietooccipital brain regions compared with frontotemporal brain regions ( $P=0.005$  and  $P=0.006$ , respectively). The percentage of positive vessels for fibrin and IgG was associated with the percentage of amyloid- $\beta$ -positive vessels (Spearman  $\rho=0.71$ ,  $P=0.015$  and Spearman  $\rho=0.73$ ,  $P=0.011$ , respectively). Moreover, the percentage of fibrin and IgG-positive vessels, but not amyloid- $\beta$ -positive vessels, was associated with the number of cerebral microbleeds on magnetic resonance imaging (Spearman  $\rho=0.77$ ,  $P=0.005$  and Spearman  $\rho=0.70$ ,  $P=0.017$ , respectively). Finally, we observed fibrin deposition in walls of vessels involved in cerebral microbleeds.

**Conclusions**—Our results raise the possibility that blood-brain barrier leakage may be a contributory mechanism for CAA-related brain injury. (*Stroke*. 2019;50:328-335. DOI: 10.1161/STROKEAHA.118.023788.)

**Key Words:** blood-brain barrier ■ cognition ■ immunohistochemistry ■ magnetic resonance imaging  
■ small vessel disease

Cerebral amyloid angiopathy (CAA) is characterized by the accumulation of amyloid- $\beta$  (A $\beta$ ) within the walls of cortical and leptomeningeal blood vessels. This type of cerebral small vessel disease is common in the aging population, found in  $\approx 33\%$  of general autopsies and up to 90% of individuals with Alzheimer disease.<sup>1,2</sup> CAA is well recognized as the most common cause of lobar intracerebral hemorrhage in the elderly<sup>3</sup> and is believed to play a fundamental role in the development of microvascular lesions, including cerebral microbleeds

(CMBs) and cerebral microinfarcts (CMIs).<sup>4,5</sup> CAA is also associated with other, more global types of brain injury, including cerebral atrophy, white matter damage, and structural network disruption.<sup>6,7</sup> Importantly, there is growing evidence that CAA has a substantial impact on age-related cognitive decline, even in the absence of lobar intracerebral hemorrhage and independent of the severity of classical Alzheimer disease pathology (ie, A $\beta$  plaques and neurofibrillary tangles).<sup>8,9</sup> This vascular cognitive impairment may result from both numerous

Received October 2, 2018; final revision received December 7, 2018; accepted December 11, 2018.

From the Department of Psychiatry and Neuropsychology, School for Mental Health and Neuroscience, Alzheimer Center Limburg, Maastricht University, the Netherlands (W.M.F., H.I.L.J.); Department of Radiology and Nuclear Medicine, School for Mental Health and Neuroscience, Maastricht University Medical Center, the Netherlands (W.M.F., W.H.B.); MassGeneral Institute for Neurodegenerative Disease (MIND), Massachusetts General Hospital, Charlestown (W.M.F., B.J.B., M.P.F., S.J.v.V.); C.S. Kubik Laboratory of Neuropathology, Department of Pathology, Massachusetts General Hospital, Boston (M.P.F.); and Department of Neurology, J. Philip Kistler Stroke Research Center (W.M.F., S.M.G., S.J.v.V.) and Division of Nuclear Medicine and Molecular Imaging, Department of Radiology (H.I.L.J.), Massachusetts General Hospital, Harvard Medical School, Boston.

The online-only Data Supplement is available with this article at <https://www.ahajournals.org/doi/suppl/10.1161/STROKEAHA.118.023788>.

Correspondence to Whitney M. Freeze, PhD, Department of Psychiatry and Neuropsychology, Maastricht University Medical Center, PO Box 616, 6200 MD Maastricht, the Netherlands. Email [whitneyfreeze@gmail.com](mailto:whitneyfreeze@gmail.com)

© 2019 American Heart Association, Inc.

*Stroke* is available at <https://www.ahajournals.org/journal/str>

DOI: 10.1161/STROKEAHA.118.023788

microvascular lesions as well as global atrophy and white matter damage, though the pathophysiology underlying CAA-related brain injuries is not well understood.

A possible role of blood-brain barrier (BBB) disruption in the cause of CAA has previously been suggested,<sup>6,10,11</sup> although experimental data demonstrating this association are lacking. The BBB is a unique feature of the cerebral microvasculature that is formed by an interactive cellular complex that involves a line-up of endothelial cells held together by tight junctions and supported by surrounding mural cells and glial cells.<sup>12</sup> Together, these cells selectively regulate molecular exchange between the blood and cerebral tissue. CAA-positive vessels exhibit several morphological changes, including loss of smooth muscle cells, luminal narrowing, and vessel wall thickening, and have been suggested to trigger inflammatory processes.<sup>3,13–16</sup> These changes likely affect the integrity of the BBB.<sup>17,18</sup> Loss of BBB integrity has been suggested as a general mechanism for small vessel disease–related brain tissue injury and vascular cognitive impairment,<sup>19</sup> but its role in the pathophysiology of CAA and CAA-related bleeding remains poorly understood.

The aim of this exploratory study was to examine pre-existing BBB leakage (which presumably occurred during life) post-mortem in cases with definite CAA, by measuring extravasation of plasma proteins fibrin and IgG within each lobe. We hypothesized that BBB leakage would be associated with CAA severity and that leakage would be increased in parietooccipital brain regions compared with frontotemporal brain regions because CAA preferentially affects the posterior lobes.<sup>20,21</sup> IgG and fibrin extravasation were quantified as the degree of vascular deposition (ie, percentage of positive vessels) and cortical fraction positive for these plasma proteins by means of immunohistochemistry. We also assessed the number of microvascular lesions (ie, CMBs and CMIs) on high-resolution post-mortem magnetic resonance imaging (MRI) and related these to markers of BBB leakage as assessed with immunohistochemistry. Finally, we explored whether markers of BBB leakage were evident near pathologically confirmed CMBs and CMIs. Seven nonneurological control cases were analyzed for comparison. The overall goal of this study was to improve our understanding of the occurrence and impact of BBB leakage in CAA as a novel potential target for treatment.

## Methods

### Data Availability Statement

The data that support the findings of this study are available from the corresponding author upon reasonable request.

### Human Brain Tissue

Intact human brain hemispheres from 11 CAA cases were received through an ongoing postmortem brain MRI study at Massachusetts General Hospital. If  $\geq 1$  large intracerebral hemorrhages were present, the least affected hemisphere was selected. Otherwise, 1 hemisphere was randomly picked. All CAA cases were patients who were diagnosed with possible or probable CAA during life<sup>22</sup> and who donated their brain or who came to autopsy through the Alzheimer's Disease Research Center as part of the Massachusetts General Hospital neuropathology service. Each patients' diagnosis was confirmed

through medical records and available clinical MRI or computed tomography obtained during life and validated upon autopsy. After autopsy, the hemispheres were fixed in 10% formalin for at least 3 weeks, before scanning. Seven control cases were received through the Massachusetts General Hospital neuropathology service and had no clinical records of neurological conditions or brain lesions during life, which was confirmed at autopsy. Two of these control cases were part of the postmortem brain MRI study, and an intact hemisphere was randomly picked for scanning. Five control cases who were not part of the postmortem MRI scanning project had undergone standard neuropathological examination and were selected based on neuropathological records. Informed consent was obtained from a legal representative before autopsy for all cases. The use of the brain specimens was in accordance with the rules and regulations of the Massachusetts General Hospital institutional review board.

### Postmortem MRI Acquisition and Analysis

Before postmortem MRI, the CAA hemispheres and 2 control hemispheres were packed in a plastic bag, filled with periodate-lysine-paraformaldehyde fixative, and vacuum sealed. The packed hemispheres were held at 4°C until the day before the MRI, when they were kept at room temperature. Any remaining air bubbles were removed, followed by resealing of the bag. Each hemisphere was subjected to postmortem MRI for the identification of CMBs<sup>23</sup> and cortical CMIs. Hemispheres were scanned overnight for  $\approx 14$  hours on a 3-T MR system (Siemens Magnetom TrioTim syngo) using a 32-channel head coil. The scan protocol included the following sequences relevant to this study: (1) T2-weighted turbo-spin echo (voxel size, 500×500×500  $\mu\text{m}^3$ ; echo time, 61 ms; repetition time, 1800 ms; flip angle, 150°; total scan time, 3 hours 8 minutes 11 seconds), and (2) gradient-echo fast low-angle shot (voxel size, 500×500×500  $\mu\text{m}^3$ ; echo time, 4.49 ms; echo time, 11.02 ms; repetition time, 20 ms; flip angle, 10°, 20°, 30°; 2 averages; total scan time, 1 hour 59 minutes). Microvascular lesions within the cortical gray matter were identified by an experienced rater (Dr van Veluw) who was blinded to CAA severity or other histopathologic findings. CMIs were defined as hyperintense cortical foci on T2-weighted images and isointense on gradient-echo images as previously described.<sup>24</sup> CMBs were counted on gradient-echo images, appearing as homogeneous round or ovoid foci of low signal intensity.<sup>25,26</sup> Because the postmortem gradient-echo sequence is susceptible to artifacts caused by remaining air bubbles between gyri, the T2-weighted scan was also visually inspected to discriminate actual CMBs from artifacts caused by air bubbles.

### Tissue Sampling

For each case, 4 cortical tissue blocks were sampled from prespecified regions within the frontal, temporal, parietal, and occipital lobe. In addition, in 1 CAA case with the highest lesion burden on MRI, an area with multiple CMBs on postmortem MRI was sampled for histopathologic examination of the vessels involved in CMBs (case no. 2, Table).

### Histopathologic Analysis

Systematically selected samples were dehydrated, embedded in paraffin, and cut into 6- $\mu\text{m}$  serial sections on a microtome. The first 2 sections of each block were stained with standard hematoxylin and eosin (to identify cortical microvascular lesions) and Luxol fast blue (to identify the white matter). Adjacent sections underwent immunohistochemistry against A $\beta$ , fibrin, and IgG. Sections were deparaffinized and rehydrated through xylene and graded series of ethanol (100%, 95%, 70%) and water. Endogenous peroxidase activity was quenched by incubating the sections in 3% hydrogen peroxide solution for 20 minutes. Antigen retrieval was performed by incubating the sections in formic acid for 5 minutes (A $\beta$  staining) or with heat-induced epitope retrieval in citrate buffer for 20 minutes (fibrin and IgG staining). Sections were blocked for 1 hour with normal horse or goat serum diluted in tris-buffered saline. Next, sections were incubated overnight at 4°C with primary antibodies against human

**Table. Case Characteristics**

Case No.	Age at Death (Years)	Sex	Postmortem Interval (Hour)	Cause of Death	Diagnosis	Cortical CAA Burden Score	A $\beta$ Plaque Score	MRI CMBs Count	Histopathology CMBs Count	MRI CMI Count	Histopathology CMI Count
1	80	M	Unknown	Unknown	CAA	5	3	41	0	115	17
2	70	M	16	ICH	CAA	9	3	261	1	33	2
3	65	M	27	Unknown	CAA	7	3	39	0	21	10
4	65	M	14	ICH	CAA	7	1	85	2	144	3
5	81	M	Unknown	Unknown	CAA	5	4	4	0	12	3
6	70	F	Unknown	Unknown	CAA	6	4	13	0	7	1
7	67	M	Unknown	Unknown	CAA	10	4	109	2	10	5
8	69	M	36	Unknown	CAA	10	4	4	0	5	0
9	64	F	30	ICH	CAA	8	4	161	0	3	3
10	79	F	37	Unknown	CAA	8	4	204	2	15	19
11	67	M	24	Unknown	CAA	5	4	55	4	27	21
12	90	M	6	Myocarditis secondary to an inflammatory syndrome	Control	0	4	0	0	3	1
13	95	F	4	Unknown	Control	0	1	1	0	1	0
14	92	M	Unknown	Unknown	Control	2	0	n/a	0	n/a	0
15	68	M	27	Multifactorial lung disease	Control	0	0	n/a	0	n/a	0
16	60	M	10	Hemorrhagic bronchopneumonia and candidemia	Control	0	0	n/a	0	n/a	0
17	76	F	39	Accidental drowning	Control	1	2	n/a	0	n/a	0
18	77	F	83	Unknown	Control	0	4	n/a	0	n/a	0

A $\beta$  indicates amyloid- $\beta$ ; CAA, cerebral amyloid angiopathy; CMB, cerebral microbleed; CMI, cerebral microinfarct; F, female; ICH, intracerebral hemorrhage; M, male; MRI, magnetic resonance imaging; and n/a, not available.

A $\beta$  (mouse monoclonal A $\beta$  [clone 6F/3D] 1:200, Dako, Denmark), human fibrin (rabbit polyclonal fibrin, 1:500, Dako, Denmark), and human IgG (rabbit polyclonal IgG, 1:500, Dako, Denmark) diluted in Tris-buffered saline. The next day a standard avidin-biotin complex method (Vectastain ABC kit from Vector Laboratories, Inc) was applied and the signal was visualized using the chromogen 3,3'-Diaminobenzidine. Between all incubation steps, sections were washed in Tris-buffered saline. Sections were counterstained with hematoxylin for 10 s, dehydrated through a series of ethanol (70%, 95%, 100%) and xylene, and cover slipped using Permount mounting medium. Negative controls were established by omitting the primary antibody, which showed no immunopositivity. The fibrin and IgG stainings were performed in 2 batches, and 3,3'-Diaminobenzidine developing time was held constant.

The additional CMBs-rich sample underwent serial sectioning as a whole. Sections  $\approx$ 200  $\mu$ m apart were stained with hematoxylin and eosin to identify individual CMBs, and the adjacent sections with A $\beta$  and fibrin, respectively, to assess protein deposition within the vessels responsible for the bleeds.

### Vascular and Parenchymal A $\beta$ Quantification

CAA burden was evaluated on A $\beta$ -stained sections by a single experienced rater (Dr van Veluw). Cortical CAA was scored using a 4-point scale; absent (0), scant A $\beta$  deposition (1), some circumferential A $\beta$  (2), and widespread circumferential A $\beta$  (3), following proposed consensus criteria.<sup>27</sup> Scores from the 4 cortical areas were added to form a single cumulative cortical CAA burden score (0–12; Table). Parenchymal A $\beta$  plaques were scored as absent (0) or present (1).

Scores from each cortical area were added to form a single cortical A $\beta$  plaque score (0–4).

### Microscopic Analyses

Sections were imaged with brightfield using the Hamamatsu NanoZoomer Digital Pathology-HT scanner (C9600-12, Hamamatsu Photonics K.K., Japan) and a  $\times$ 20 objective. The viewing platform NDP.View (version 2.6.13) was used to analyze the digital sections. For the analysis of vascular protein deposition, three 3 $\times$ 3 mm<sup>2</sup> rectangular regions of interest (ROIs) were manually placed at random locations within the cortex on each digital section (A $\beta$ -, fibrin-, and IgG-stained sections; Figure I in the [online-only Data Supplement](#)). Caution was taken to omit damaged areas on the sections, and the ROIs were placed while blinded to pathology burden at low magnification ( $\times$ 0.16). CMIs or CMBs, if present, were not included in ROIs. ROI placement was guided by the Luxol fast blue-stained section to assure correct positioning within cortical tissue. Within the ROIs, the number of vessels that were positive and negative for CAA, fibrin, or IgG was counted by a single rater (Dr Freeze). Cortical vessels  $\leq$ 20  $\mu$ m and all leptomeningeal vessels were excluded. Vessels were regarded as positive when clear immunoreactivity against A $\beta$ , fibrin, or IgG was evident within the vessel wall, but not when immunoreactivity was only apparent within the lumen. To quantify the number of cortical vessels positive for CAA, fibrin, or IgG, the percentage of immunopositive vessels versus the total number of vessels analyzed was determined. This method was applied to calculate the percentage of positive vessels within the frontotemporal cortex, the parietooccipital cortex, and within all lobes combined. We also computed a

weighted whole brain score which was corrected for differences in lobar volumes based on previously reported mean lobar volumes from 70- to 85-year-old nondemented individuals.<sup>28</sup> To calculate the weighted score, the number of positive and negative vessels was multiplied by the relative volume fraction of the corresponding lobe. A second rater (Dr van Veluw) independently rated the number of positive and negative vessels on 27 randomly selected ROIs. Both raters were blinded to clinical and MRI information and brain region.

The cortical area fraction positive for IgG or fibrin was determined using digital image analysis with ImageJ free software (FIJI version 2.0.0).<sup>29</sup> The percent area fraction of fibrin and IgG labeling of cortical gray matter was determined using image thresholding (Methods and Figure II in the [online-only Data Supplement](#)). The average percent positive area of the frontal and temporal lobe was taken as frontotemporal score and the average percent positive area of the parietal and occipital lobe as parietooccipital score.

CMI and CMBs were evaluated by a single experienced rater (Dr van Veluw) on the hematoxylin and eosin-stained sections. CMIs were defined as areas of tissue pallor, with evidence of cell loss and gliosis. CMBs were identified by evidence of erythrocyte extravasation (ie, acute CMBs) or blood breakdown products including hematoxylin or hemosiderin (ie, subacute CMBs).<sup>23</sup>

## Statistical Analysis

A threshold of  $\alpha < 0.05$  was used to determine statistical significance. Interrater reliability was determined using the intraclass correlation coefficient based on a single rating, absolute agreement 2-way random effects model.<sup>30</sup> We assessed differences on the BBB leakage measures between CAA cases and controls using Mann-Whitney *U* tests. Wilcoxon-signed rank tests were applied to assess differences in BBB leakage measures in frontotemporal compared with parietooccipital brain regions within the CAA cases. Associations between continuous variables were determined with bivariate and partial Spearman  $\rho$  correlation coefficients. All *P* are 2-tailed, and we did not correct for multiple comparisons because this was an exploratory study. Therefore, the results should be considered as hypothesis generating. All analyses were conducted with R statistical software (R version 3.3.3).<sup>31</sup>

## Results

Characteristics for each case are listed in Table. The median (interquartile range) age at death of the 11 CAA cases was 69 years (65–79 years), and 8 were male. The median (interquartile range) age at death of the 7 control cases was 77 years (68–92 years), and 4 were male. A $\beta$  plaque scores were higher in CAA cases compared with controls ( $P=0.037$ ), but there were

no significant group differences with regard to age at death ( $P=0.17$ ) and postmortem interval ( $P=0.67$ ). The percentage of positive vessels for A $\beta$  was higher in CAA cases compared with controls in the frontotemporal ( $P=0.006$ ) and parietooccipital ( $P<0.001$ ) cortices and in the parietooccipital cortex compared with the frontotemporal cortex within CAA cases ( $P=0.024$ ), which is consistent with the predilection of CAA for posterior brain regions (Figure III in the [online-only Data Supplement](#)). Age at death was negatively associated with the percentage of vessels positive for fibrin (Spearman  $\rho=-0.54$ ,  $P=0.022$ ) and IgG (Spearman  $\rho=-0.52$ ,  $P=0.025$ ) when both cases and controls were included in the analysis, but the associations were not significant when the groups were analyzed separately (all  $P>0.05$ ). Postmortem interval and A $\beta$  plaque score were not significantly associated with extravasation of IgG or fibrin (all  $P>0.05$ ). We did not observe any obvious batch effects with regard to the BBB leakage measures. Interrater reliability for the assessment of the number of positive vessels ( $n=27$  regions) was good to excellent (intraclass correlation coefficient, 0.894; 95% CI, 0.77–0.95; range number of positive vessels within ROIs, 0–65) and for the assessment of the number of negative vessels poor to moderate (intraclass correlation coefficient, 0.248; 95% CI=-0.10–0.60; range number of negative vessels within ROIs, 0–34).

## Cortical Area Percentage Positive for Plasma Proteins

The cortical area percentage positive for IgG within both the frontotemporal and the parietooccipital cortex was higher in CAA cases compared with controls (frontotemporal,  $P=0.044$ ; parietooccipital,  $P=0.001$ ; Figure 1). Within the CAA cases, the cortical area percentage positive for fibrin and IgG was higher in parietooccipital brain regions compared with frontotemporal brain regions (Fibrin,  $P=0.005$ ; IgG,  $P=0.006$ ; Figure 1).

## Percentage of Positive Vessels for Plasma Proteins

The percentage of positive vessels for IgG was higher in CAA cases compared with controls in the parietooccipital

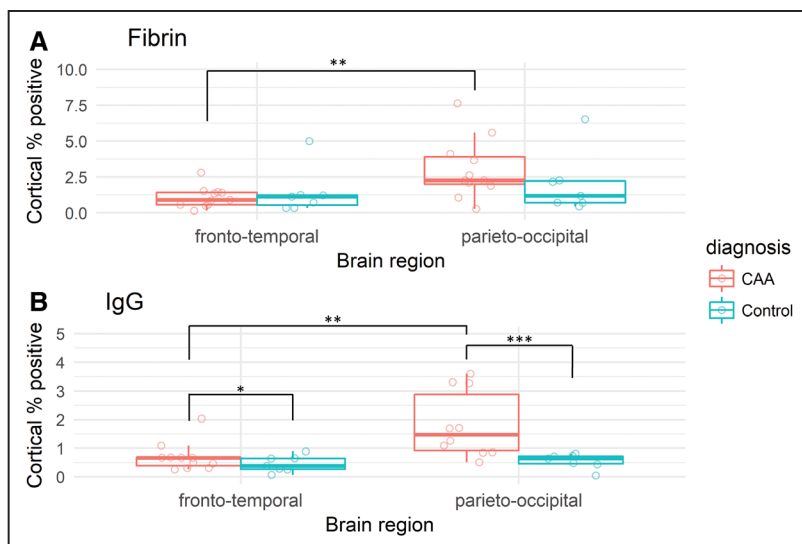


**Figure 1.** Percentage of cortical area positive for fibrin or IgG. Percentage of cortical area positive for fibrin (A) and IgG (B) within cerebral amyloid angiopathy (CAA) cases ( $n=11$ ) and controls ( $n=7$ ). Cortical positivity for IgG was higher in CAA cases compared with controls in both frontotemporal and parietooccipital brain regions. Within CAA cases, the cortical percentage positive for fibrin and IgG was higher in parietooccipital brain regions compared with frontotemporal brain regions. (Mann-Whitney *U* tests were applied for between-case comparisons and Wilcoxon signed-rank tests for within-case comparisons; \* $P<0.05$ ; \*\* $P<0.01$ , \*\*\* $P<0.001$ ).

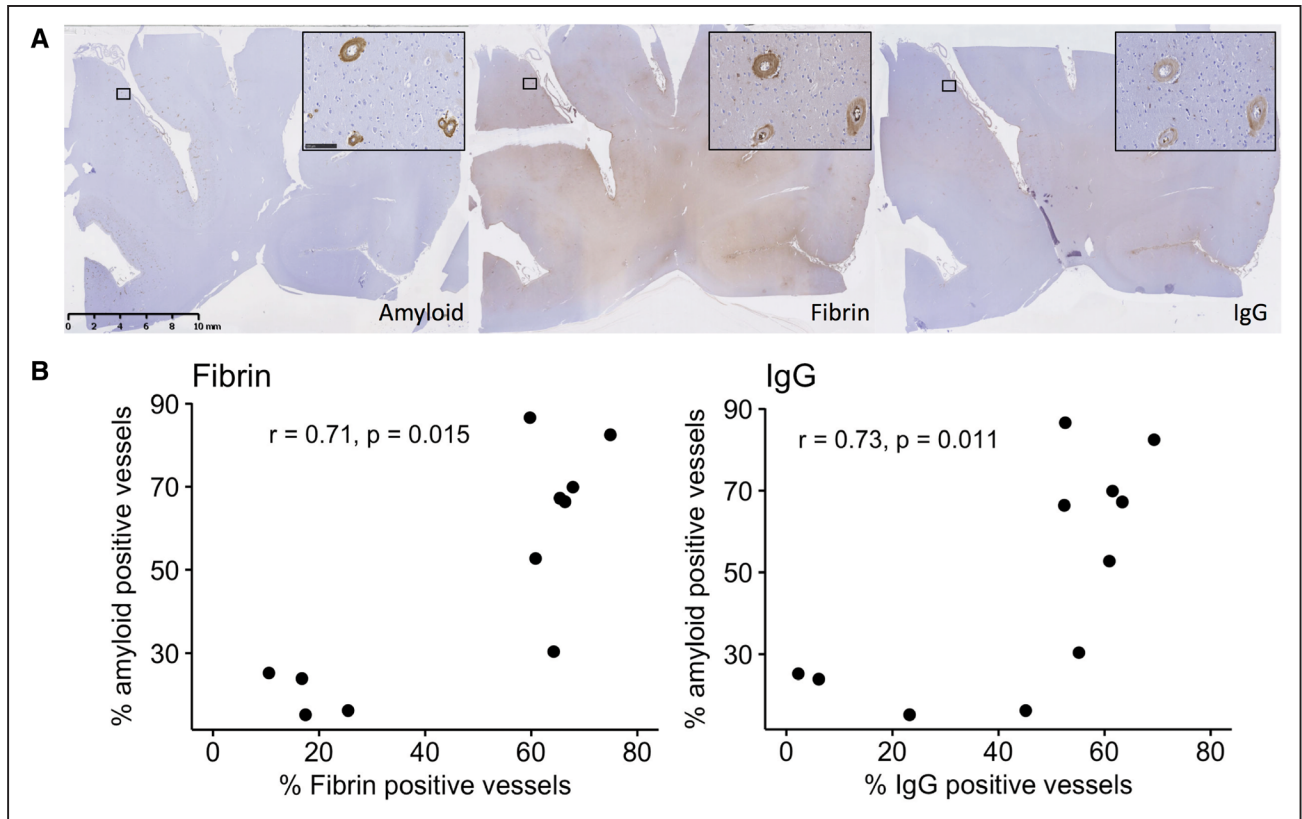


**Figure 2.** Immunohistochemistry against amyloid- $\beta$  ( $A\beta$ ), fibrin, and IgG was performed on cortical brain sections, and the percentage of positive vessels was determined. **A**, Representative images of  $A\beta$ , fibrin, and IgG staining in CAA case no. 2. **B**, Associations (Spearman rank correlations) between whole brain percentage of cortical vessels positive for  $A\beta$  and whole brain percentage of cortical vessels positive for fibrin and IgG. Only CAA cases ( $n=11$ ) were included in the analyses. Scale bar sections=10 mm, scale bar inset=100  $\mu$ m.

cortex ( $P=0.022$ ). Within the CAA cases, there was a higher percentage of vessels positive for IgG in the parietooccipital cortex compared with the frontotemporal cortex ( $P=0.004$ ; Figure III in the [online-only Data Supplement](#)).

### CAA Severity and Leakage Markers

Within CAA cases, the percentage of  $A\beta$ -positive vessels within all lobes combined was associated with the percentage vessels positive for fibrin (Spearman  $\rho=0.71$ ,  $P=0.015$ ) and IgG (Spearman  $\rho=0.73$ ,  $P=0.011$ ) within all lobes combined (Figure 2). We found similar results when we weighted the percentage of positive vessels to account for differences in

lobar volumes. Moreover, the results did not notably change when we corrected for age at death and plaque score.

### Microvascular Lesions and Leakage Markers

The number of CMBs counted on MRI was positively associated with the percentage of fibrin (Spearman  $\rho=0.77$ ,  $P=0.005$ ) and IgG (Spearman  $\rho=0.70$ ,  $P=0.017$ ) positive vessels within all lobes combined, but not with the percentage of  $A\beta$ -positive vessels within all lobes combined (Spearman  $\rho=0.32$ ,  $P=0.33$ ; Figure 3). No significant associations were found between the number of CMBs counted on MRI and the percentage of fibrin (Spearman  $\rho=-0.12$ ,  $P=0.73$ ), IgG (Spearman  $\rho=0.17$ ,

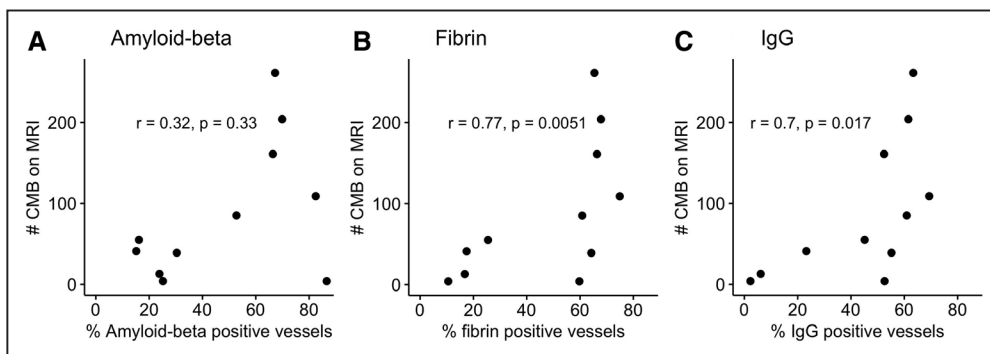


**Figure 3.** Number of cerebral microbleeds (CMBs) against percentage vessels positive for plasma proteins and amyloid- $\beta$  ( $A\beta$ ). Data points representing the percentage of positive vessels across all lobes for (A)  $A\beta$ , (B) fibrin, and (C) IgG, against number of CMBs rated on postmortem magnetic resonance imaging (MRI). Spearman rank correlations with corresponding  $P$  are depicted in each graph. Only CAA cases ( $n=11$ ) were included in the analyses.

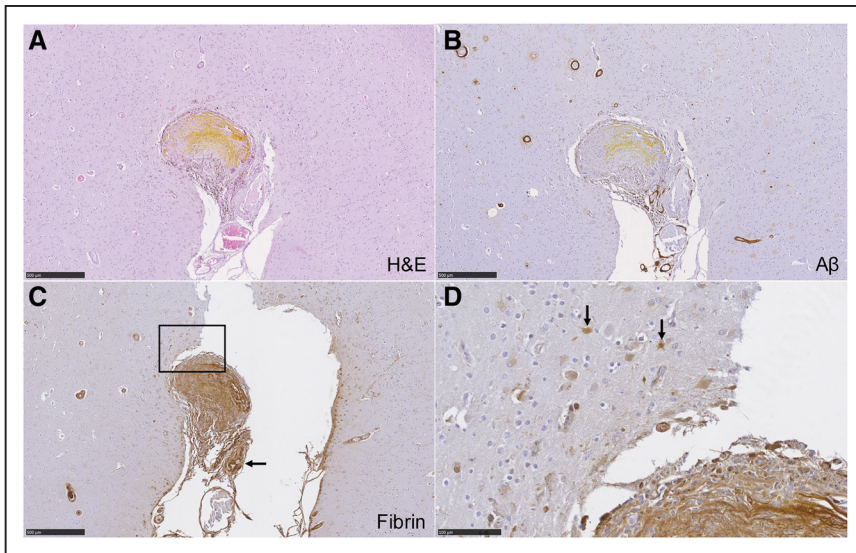


**Figure 4.** Blood-brain barrier leakage surrounding a cerebral microbleed (CMB). A microbleed observed on postmortem magnetic resonance imaging (MRI) in case no. 2 was sampled for histopathologic analysis (**A**, hematoxylin and eosin [H&E] stain). Fibrin deposition (**C**), but not amyloid- $\beta$  ( $A\beta$ ) accumulation (**B**), was present in the wall of the vessel that was involved in the CMBs. Note that fibrin accumulation was not only observed at the site of bleeding, but also in the wall of the unruptured part of the vessel (arrow). On the magnified image, immunopositivity for fibrin can be observed in astrocytes surrounding the lesion (**D**; arrows). Scale bars in **A**, **B**, and **C** are 500  $\mu$ m, **D**=100  $\mu$ m.

$P=0.61$ ), or  $A\beta$ -positive vessels (Spearman  $\rho=-0.41$ ,  $P=0.21$ ). We found similar results when we weighted the percentage of positive vessels to account for differences in lobar volumes. When the analyses were corrected for age at death and plaque score, the association between CMBs counted on MRI and the percentage of vessels positive for IgG became marginally significant (partial Spearman  $\rho=0.66$ ,  $P=0.051$ ).

#### Plasma Proteins Near Microvascular Lesions

Histopathologic examination of CMBs revealed fibrin deposition within the walls of the involved vessel (Figure 4) and fibrin uptake in neurons and astrocytes surrounding the hemorrhagic lesions. Cellular uptake of fibrin and IgG was not associated with CMIs.

### Discussion

The aim of this exploratory postmortem study was to evaluate whether BBB disruption might play a role in CAA-related brain injury by assessing associations between markers of BBB disruption, CAA severity, and microvascular lesions. Our data show higher cortical and vascular positivity for plasma proteins in CAA cases compared with controls, with a posterior predilection within CAA cases. Importantly, cerebrovascular deposition of plasma proteins was positively associated with CAA severity itself and with total number of CMBs detected on MRI, whereas CAA severity was not significantly associated with number of CMBs. Histological examination of microvascular lesions showed fibrin deposition within the wall of vessels presumably involved in microhemorrhage.

Plasma protein extravasation and cellular uptake of plasma proteins have been previously demonstrated in normal aging, cerebral small vessel disease, and Alzheimer disease.<sup>32-34</sup> We observed a negative association between vascular plasma protein deposition and age at death when both CAA cases and controls were included in the analyses, which might be explained by the relatively high age and low pathology within the control group. We observed higher cortical and vascular IgG positivity in CAA cases compared with controls, despite the controls being on average older (mean age, 80 years)

than the CAA cases (mean age, 71 years). Furthermore, the higher cortical and vascular plasma protein positivity in the parietooccipital cortex compared with the frontotemporal cortex within CAA cases is in line with the predilection of CAA pathology and associated lesions for posterior brain regions.<sup>20,21</sup> The observed immunolabeling of fibrin within cells surrounding CMBs on the one hand suggests that extravasated plasma proteins can be absorbed by local neurons and glial cells, which could be a contributing factor to altered structural connectivity in CAA.<sup>35</sup> Leakage of plasma proteins within the vessel wall, on the other hand, may be a contributory mechanism to vessel wall thickening, impaired autoregulation, and altered vascular reactivity in CAA.

Our results are consistent with previous observations showing more frequent plasma protein deposition within CAA-positive vessels compared with normal vessels.<sup>17,36</sup> Interestingly, vascular deposition of fibrin and IgG was positively related to the number of CMBs on postmortem MRI, whereas vascular deposition of  $A\beta$  (measured as the percentage of  $A\beta$ -positive vessels) was not. This raises the question as to whether vascular  $A\beta$  is directly (as frequently assumed) or indirectly (through its association with BBB disruption) involved in CMBs formation.<sup>37</sup> Because the BBB provides protection against red blood cell extravasation, CMBs might represent an extreme form of BBB disruption.<sup>38</sup> BBB leakage of plasma proteins may therefore form a potential biomarker to identify vessels at risk for rupture. If confirmed, this mechanism could generate new treatment strategies or methods for monitoring bleeding risk and treatment response.

Strengths of this study are the use of postmortem MRI scans of intact hemispheres of well-characterized cases to assess microvascular lesions throughout the brain. Because CMBs often escape detection on routine histopathologic examination (in contrast to CMIs), we added additional serial sections from 1 case exhibiting many CMBs on MRI, which may not be generalizable to other cases. Another limitation is the fact that the postmortem interval was unknown for 5 cases. However, this study as well as previous studies in larger samples found no significant associations between plasma protein extravasation and postmortem interval.<sup>17,32</sup> Although we

corrected for plaque score and age at death in the correlation analyses, we were not able to do the same for between-group comparisons because of the nonparametric nature of the analyses. Finally, the poor to moderate interrater agreement of the assessment of negative vessels may have resulted in variability or bias. Further larger studies including longitudinal in vivo imaging data in patients with CAA are warranted to address the question whether BBB disruption could be an early marker in CAA-related brain injury.

### Conclusions

This study revealed positive associations between markers of BBB leakage and CAA severity. Moreover, BBB leakage, but not CAA severity, was associated with CMBs. Our observations suggest that BBB disruption might play a fundamental role in the pathogenesis of CAA-related brain injury and thus represents a target for future interventions aimed at preventing cognitive impairment and lesion formation in CAA.

### Sources of Funding

This work was supported by Alzheimer Nederland and Stichting 2Bike4Alzheimer (research grant WE-03-2012-40; Dr Freeze). Dr van Veluw received funding from the Netherlands Organisation for Scientific Research (Rubicon fellowship 019.153LW.014). Drs Bacskai, Frosch, and Greenberg received funding from the National Institutes of Health (R01 NS096730).

### Disclosures

None.

### References

- Jellinger KA, Attems J. Prevalence and pathogenic role of cerebrovascular lesions in Alzheimer disease. *J Neurol Sci*. 2005;229-230:37-41. doi: 10.1016/j.jns.2004.11.018
- Maia LF, Mackenzie IR, Feldman HH. Clinical phenotypes of cerebral beta-amyloid angiopathy. *J Neurol Sci*. 2007;257:23-30. doi: 10.1016/j.jns.2007.01.054
- Vinters HV. Cerebral amyloid angiopathy. A critical review. *Stroke*. 1987;18:311-324.
- Soontornniyomkij V, Lynch MD, Mermash S, Pomakian J, Badkoobehi H, Clare R, et al. Cerebral microinfarcts associated with severe cerebral beta-amyloid angiopathy. *Brain Pathol*. 2010;20:459-467. doi: 10.1111/j.1750-3639.2009.00322.x
- Olichney JM, Ellis RJ, Katzman R, Sabbagh MN, Hansen L. Types of cerebrovascular lesions associated with severe cerebral amyloid angiopathy in Alzheimer's disease. *Ann N Y Acad Sci*. 1997;826:493-497.
- Charidimou A, Boulouis G, Gurol ME, Ayata C, Bacskai BJ, Frosch MP, et al. Emerging concepts in sporadic cerebral amyloid angiopathy. *Brain*. 2017;140:1829-1850. doi: 10.1093/brain/awx047
- Smith EE. Cerebral amyloid angiopathy as a cause of neurodegeneration. *J Neurochem*. 2018;144:651-658. doi: 10.1111/jnc.14157
- Greenberg SM, Gurol ME, Rosand J, Smith EE. Amyloid angiopathy-related vascular cognitive impairment. *Stroke*. 2004;35(11 suppl 1):2616-2619. doi: 10.1161/01.STR.0000143224.36527.44
- Arvanitakis Z, Leurgans SE, Wang Z, Wilson RS, Bennett DA, Schneider JA. Cerebral amyloid angiopathy pathology and cognitive domains in older persons. *Ann Neurol*. 2011;69:320-327. doi: 10.1002/ana.22112
- Fisher M, French S, Ji P, Kim RC. Cerebral microbleeds in the elderly: a pathological analysis. *Stroke*. 2010;41:2782-2785. doi: 10.1161/STROKEAHA.110.593657
- van Nieuwenhuizen KM, Hendrikse J, Klijn CJM. New microbleed after blood-brain barrier leakage in intracerebral haemorrhage. *BMJ Case Rep*. 2017;2017. doi: 10.1136/bcr-2016-218794
- Zhao Z, Nelson AR, Betsholtz C, Zlokovic BV. Establishment and dysfunction of the blood-brain barrier. *Cell*. 2015;163:1064-1078. doi: 10.1016/j.cell.2015.10.067
- Greenberg SM, Vonsattel JP. Diagnosis of cerebral amyloid angiopathy. Sensitivity and specificity of cortical biopsy. *Stroke*. 1997;28:1418-1422.
- Vonsattel JP, Myers RH, Hedley-Whyte ET, Ropper AH, Bird ED, Richardson EP Jr. Cerebral amyloid angiopathy without and with cerebral hemorrhages: a comparative histological study. *Ann Neurol*. 1991;30:637-649.
- Matsuo K, Shindo A, Niwa A, Tabei KI, Akatsu H, Hashizume Y, et al. Complement activation in capillary cerebral amyloid angiopathy. *Dement Geriatr Cogn Disord*. 2017;44:343-353. doi: 10.1159/000486091
- Zabel M, Schrag M, Crofton A, Tung S, Beaufond P, Van Ornam J, et al. A shift in microglial  $\beta$ -amyloid binding in Alzheimer's disease is associated with cerebral amyloid angiopathy. *Brain Pathol*. 2013;23:390-401. doi: 10.1111/bpa.12005
- Hultman K, Strickland S, Norris EH. The APOE  $\epsilon$ 4/ $\epsilon$ 4 genotype potentiates vascular fibrin(ogen) deposition in amyloid-laden vessels in the brains of Alzheimer's disease patients. *J Cereb Blood Flow Metab*. 2013;33:1251-1258. doi: 10.1038/jcbfm.2013.76
- Hernandez-Guillamon M, Martinez-Saez E, Delgado P, Domingues-Montanari S, Boada C, Penalba A, et al. MMP-2/MMP-9 plasma level and brain expression in cerebral amyloid angiopathy-associated hemorrhagic stroke. *Brain Pathol*. 2012;22:133-141. doi: 10.1111/j.1750-3639.2011.00512.x
- Wardlaw JM, Sandercock PA, Dennis MS, Starr J. Is breakdown of the blood-brain barrier responsible for lacunar stroke, leukoaraiosis, and dementia? *Stroke*. 2003;34:806-812. doi: 10.1161/01.STR.0000058480.77236.B3
- Rosand J, Muzikansky A, Kumar A, Wisco JJ, Smith EE, Betensky RA, et al. Spatial clustering of hemorrhages in probable cerebral amyloid angiopathy. *Ann Neurol*. 2005;58:459-462. doi: 10.1002/ana.20596
- Vinters HV, Gilbert JJ. Cerebral amyloid angiopathy: incidence and complications in the aging brain. II. The distribution of amyloid vascular changes. *Stroke*. 1983;14:924-928.
- Greenberg SM, Charidimou A. Diagnosis of cerebral amyloid angiopathy: evolution of the Boston criteria. *Stroke*. 2018;49:491-497. doi: 10.1161/STROKEAHA.117.016990
- van Veluw SJ, Charidimou A, van der Kouwe AJ, Lauer A, Reijmer YD, Costantino I, et al. Microbleed and microinfarct detection in amyloid angiopathy: a high-resolution MRI-histopathology study. *Brain*. 2016;139(pt 12):3151-3162. doi: 10.1093/brain/aww229
- van Veluw SJ, Shih AY, Smith EE, Chen C, Schneider JA, Wardlaw JM, et al. Detection, risk factors, and functional consequences of cerebral microinfarcts. *Lancet Neurol*. 2017;16:730-740. doi: 10.1016/S1474-4422(17)30196-5
- Gregoire SM, Chaudhary UJ, Brown MM, Yousry TA, Kallis C, Jäger HR, et al. The Microbleed Anatomical Rating Scale (MARS): reliability of a tool to map brain microbleeds. *Neurology*. 2009;73:1759-1766. doi: 10.1212/WNL.0b013e3181c34a7d
- Wardlaw JM, Smith EE, Biessels GJ, Cordonnier C, Fazekas F, Frayne R, et al. Standards for Reporting Vascular changes on neuroimaging (STRIVE v1). Neuroimaging standards for research into small vessel disease and its contribution to ageing and neurodegeneration. *Lancet Neurol*. 2013;12:822-838. doi: 10.1016/S1474-4422(13)70124-8
- Love S, Chalmers K, Ince P, Esiri M, Attems J, Jellinger K, et al. Development, appraisal, validation and implementation of a consensus protocol for the assessment of cerebral amyloid angiopathy in post-mortem brain tissue. *Am J Neurodegener Dis*. 2014;3:19-32.
- Resnick SM, Goldszal AF, Davatzikos C, Golski S, Kraut MA, Metter EJ, et al. One-year age changes in MRI brain volumes in older adults. *Cereb Cortex*. 2000;10:464-472.
- Schindelin J, Arganda-Carreras I, Frise E, Kaynig V, Longair M, Pietzsch T, et al. Fiji: an open-source platform for biological-image analysis. *Nat Methods*. 2012;9:676-682. doi: 10.1038/nmeth.2019
- Koo TK, Li MY. A guideline of selecting and reporting intraclass correlation coefficients for reliability research. *J Chiropr Med*. 2016;15:155-163. doi: 10.1016/j.jcm.2016.02.012
- R Development Core Team. *A Language and Environment for Statistical Computing*. Vienna, Austria: R Foundation for Statistical Computing; 2016.
- Bridges LR, Andoh J, Lawrence AJ, Khoong CHL, Poon W, Esiri MM, et al. Blood-brain barrier dysfunction and cerebral small vessel disease (arteriolosclerosis) in brains of older people. *J Neuropathol Exp Neurol*. 2014;73:1026-1033. doi: 10.1097/NEN.0000000000000124
- Hainsworth AH, Minnett T, Andoh J, Forster G, Bhide I, Barrick TR, et al. Neuropathology of white matter lesions, blood-brain



- barrier dysfunction, and dementia. *Stroke*. 2017;48:2799–2804. doi: 10.1161/STROKEAHA.117.018101
34. Viggars AP, Wharton SB, Simpson JE, Matthews FE, Brayne C, Savva GM, et al. Alterations in the blood brain barrier in ageing cerebral cortex in relationship to Alzheimer-type pathology: a study in the MRC-CFAS population neuropathology cohort. *Neurosci Lett*. 2011;505:25–30. doi: 10.1016/j.neulet.2011.09.049
  35. Reijmer YD, Fotiadis P, Charidimou A, van Veluw SJ, Xiong L, Riley GA, et al. Relationship between white matter connectivity loss and cortical thinning in cerebral amyloid angiopathy. *Hum Brain Mapp*. 2017;38:3723–3731.
  36. Cortes-Canteli M, Paul J, Norris EH, Bronstein R, Ahn HJ, Zamolodchikov D, et al. Fibrinogen and beta-amyloid association alters thrombosis and fibrinolysis: a possible contributing factor to Alzheimer's disease. *Neuron*. 2010;66:695–709. doi: 10.1016/j.neuron.2010.05.014
  37. van Veluw SJ, Kuijf HJ, Charidimou A, Viswanathan A, Biessels GJ, Rozemuller AJ, et al. Reduced vascular amyloid burden at microhemorrhage sites in cerebral amyloid angiopathy. *Acta Neuropathol*. 2017;133:409–415. doi: 10.1007/s00401-016-1635-0
  38. Fisher M. Cerebral microbleeds and thrombolysis: clinical consequences and mechanistic implications. *JAMA Neurol*. 2016;73:632–635. doi: 10.1001/jamaneurol.2016.0576